

**INTERNATIONAL COUNCIL FOR RESEARCH AND INNOVATION
IN BUILDING AND CONSTRUCTION**

WORKING COMMISSION W18 - TIMBER STRUCTURES

SELF-TAPPING SCREWS AS REINFORCEMENTS IN BEAM SUPPORTS

I Bejtka

H J Blaß

Lehrstuhl für Ingenieurholzbau und Baukonstruktionen
Universität Karlsruhe

GERMANY

MEETING THIRTY-NINE

FLORENCE

ITALY

AUGUST 2006

Self-tapping screws as reinforcements in beam supports

I. Bejtka, H.J. Blaß

Lehrstuhl für Ingenieurholzbau und Baukonstruktionen

Universität Karlsruhe, Germany

1 Introduction

The compressive strength of timber perpendicular to the grain is much lower than the respective strength value parallel to the grain. The ratio of the characteristic compressive strength perpendicular to the grain to the compressive strength parallel to the grain for solid timber is about 1/8. Particularly beam supports should hence be detailed in order to minimise compressive stresses perpendicular to the grain.

Increasing the load-carrying capacity of beam supports may be obtained by enlarging the area loaded perpendicular to the grain or by reinforcing the beam support area. Self-tapping screws with continuous threads represent a simple and economic reinforcement method. The screws are placed at the beam support perpendicular to the grain direction. To evenly apply the support load on the screws and on the timber, a steel plate is placed between the beam surface and the support.

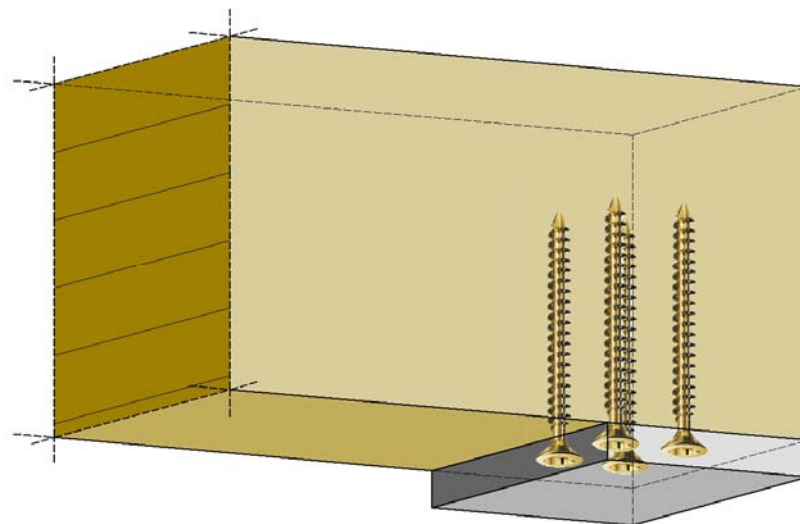


Fig. 1: Bottom view of a reinforced beam support

Comparing the test results, the load-carrying capacity of reinforced beam supports was at maximum 300% higher than the load-carrying capacity of non-reinforced beam supports.

The maximum ratio between the stiffness perpendicular to the grain of reinforced beam supports and the corresponding stiffness of non-reinforced beam supports was about 5.

To calculate the load-carrying capacity and to estimate the stiffness of reinforced beam supports two calculation models were derived. In this paper both calculation models will be presented.

2 Calculation model for the load-carrying capacity

2.1 Assumptions

The load-carrying capacity reinforced beam supports is calculated taking into account three different failure modes. The governing failure mode depends primarily on the geometry of the beam support and on the geometry of the reinforcing screws i.e. their slenderness ratio. Further parameters influencing the load-carrying capacity are the number and the yield strength of the screws and the strength class of the timber.

The first failure mode occurs in reinforced beam supports with a low number of short screws. In this case, the load-carrying capacity of the reinforced beam support is characterised by pushing the screws into the timber. Simultaneously, the compressive strength perpendicular to the grain at the contact surface is reached. For screws the pushing-in capacity is considered equal to the withdrawal capacity.

The second failure mode occurs in beam supports with slender screws. Here, the reinforcing screws are prone to buckle. Simultaneously, as in the first failure mode, the compressive strength perpendicular to the grain at the contact surface is reached. A typical buckling shape of slender reinforcing screws is shown left in *Fig. 2*.

The third and last failure mode is observed in beam supports with multiple short screws. Here, the load-carrying capacity of the reinforced beam support is characterised by reaching the compressive strength of timber perpendicular to the grain in a plane formed by the screw tips (right in *Fig. 2*).

Taking into account the three possible failure modes, the pushing-in capacity and the buckling load of the reinforcing screws and the compressive strength perpendicular to the grain at the contact surface as well as in a plane formed by the screw tips affect the load-carrying capacity of reinforced beam supports. The compressive strength perpendicular to the grain at the contact surface may be calculated according to [4] (see also in [1]). The pushing-in capacity and the buckling load of the reinforcing screw as well as the compressive strength perpendicular to the grain in a plane formed by the screw tips are presented subsequently.

For the first two failure modes it is assumed, that the compressive strength perpendicular to the grain at the contact surface of the beam and the load-carrying capacity of the axially loaded screws are reached at the same time. For the compressive strength perpendicular to the grain a linear-elastic - ideal-plastic and for the axially loaded screw a linear-elastic load-displacement behaviour is adopted. In spite of different load-displacement behaviour, numerical and analytical calculations confirm that the load-carrying capacity of the axially loaded screws is reached when the compressive strength of the timber is already reached. For this reason, both load-carrying capacities can be added to calculate the load-carrying capacity of reinforced beam supports.

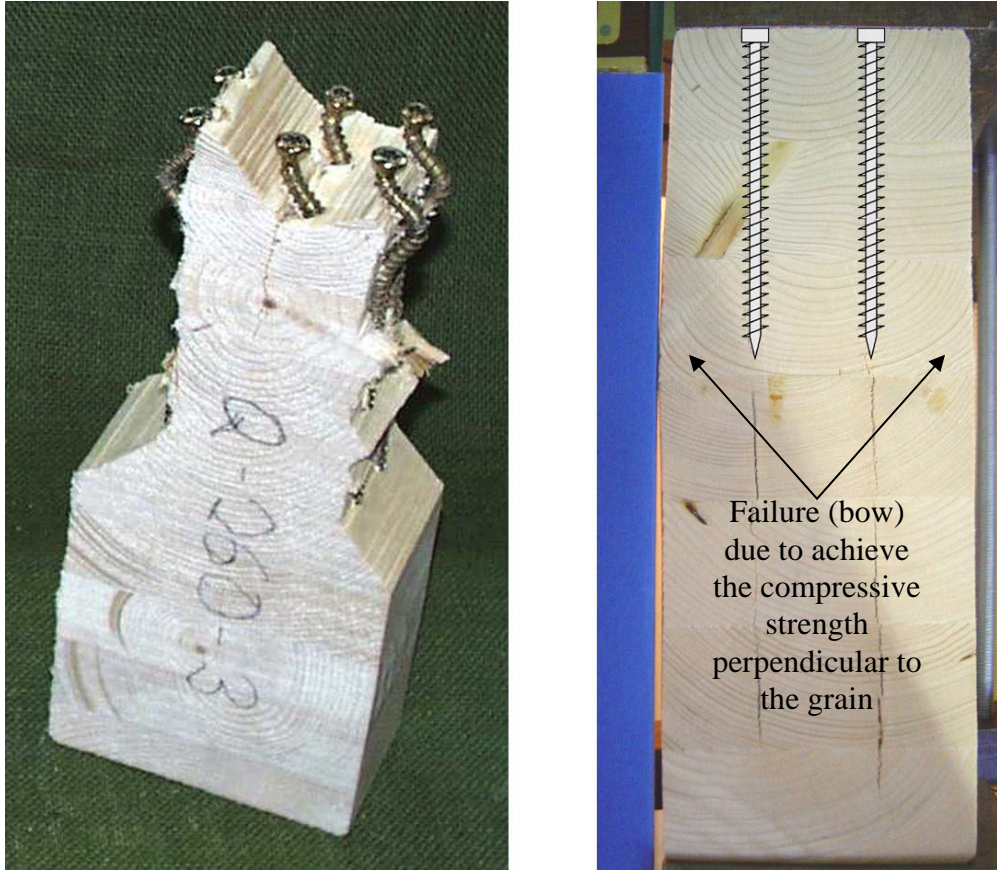


Fig. 2: Buckling of the screws and timber failure in a plane formed by the screw tips

2.2 Pushing-in capacity of self-tapping screws

Preliminary tests have confirmed, that the pushing-in capacity of self-tapping screws is equal to the withdrawal capacity R_{ax} . To determine the pushing-in capacity, 413 withdrawal tests with self-tapping screws were performed. Here, the screw diameter d between 6 and 12 mm and the penetration length of the screw l_s in the timber between $3,33 \cdot d$ and $16 \cdot d$ were varied. The angle between the screw axis and the grain direction was 90° . The best correlation between the test results and the calculated values can be achieved, when the withdrawal capacity is calculated by the following equation.

$$R_{ax} = 0,6 \cdot \sqrt{d} \cdot l_s^{0,9} \cdot \rho^{0,8} \quad (1)$$

The best correlation between characteristic values and test results can be achieved by replacing the factor 0,6 by 0,56 in eq. (1) (see Fig. 3).

In Fig. 3 the calculated characteristic withdrawal capacities in comparison to the test results are displayed.

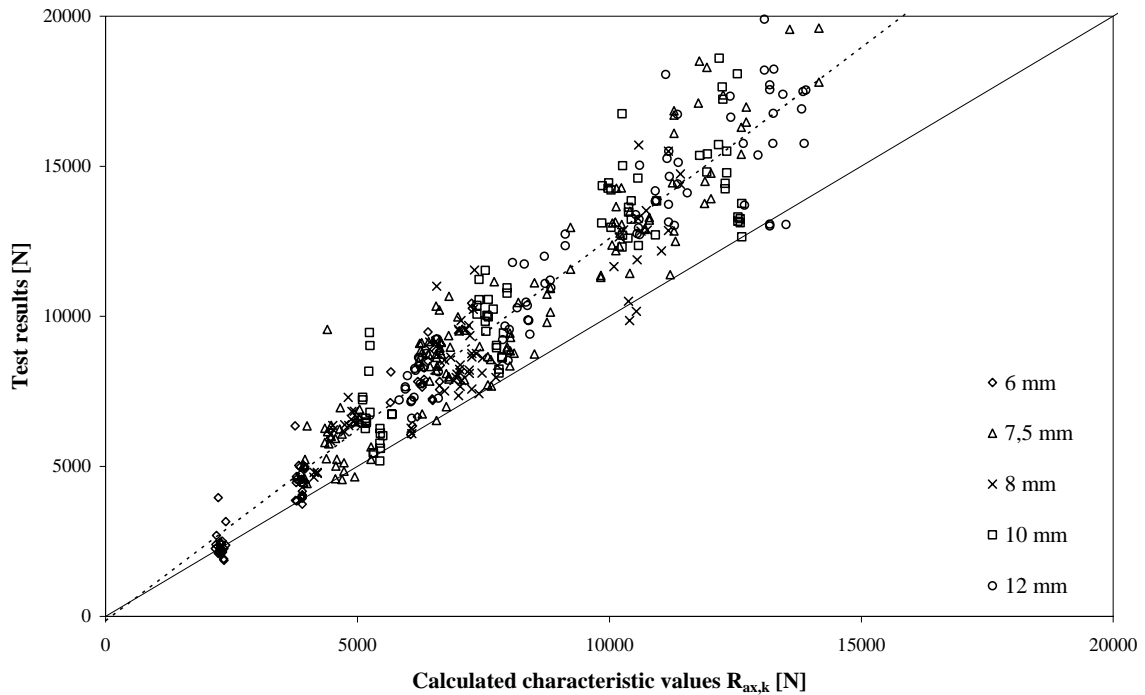


Fig. 3: Calculated characteristic withdrawal capacities in comparison to the test results

2.3 Buckling load of self-tapping screws as reinforcements

The second failure mode is characterised by screw buckling. Here, the reinforcing screws are axially loaded in compression. The ultimate load-carrying capacity for buckling of screws with a circular cross section can be calculated taking into account amongst others the buckling load. The buckling load for axially loaded screws, which are embedded in the timber, was determined by a numerical model (Fig. 4).

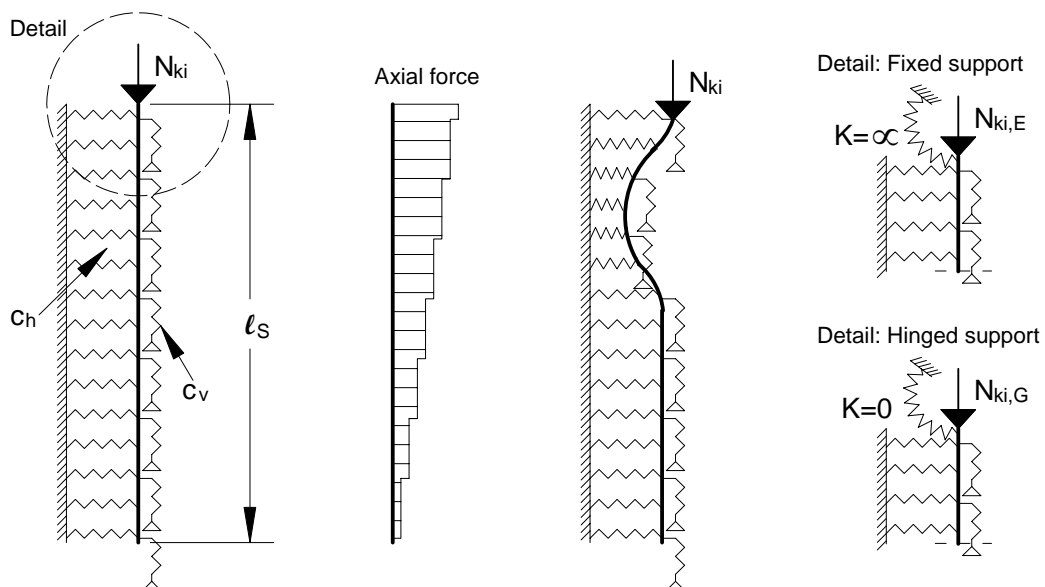


Fig. 4: Numerical model to determine the buckling load N_{ki}

The axially loaded screw with the elastic foundation c_h and with the elastic support c_v is displayed left in *Fig. 4*. The elastic foundation c_h was determined from tests to determine the embedding strength of the timber loaded by screws (400 tests). The elastic support c_v was determined from tests to determine the withdrawal or pushing-in capacity of the screws (300 tests).

The best correlation between the test results and the calculated values can be achieved, when the elastic foundation c_h is calculated by the following equation.

$$c_h = \frac{(0,22 + 0,014 \cdot d) \cdot \rho}{1,17 \cdot \sin^2 \alpha + \cos^2 \alpha} \quad (2)$$

The angle α is the angle between the grain and the force direction. For $\alpha = 90^\circ$ the elastic foundation is smaller than the representative value for an angle of 0° . Hence, reinforcing screws bedded into the timber are prone to buckle perpendicular to the grain.

For the elastic support c_v , the best correlation between the test results and the calculated values can be achieved, when the elastic support c_v is calculated by the following equation.

$$c_v = 234 \cdot \frac{(\rho \cdot d)^{0,2}}{\ell_s^{0,6}} \quad (3)$$

The distribution of the axial force (*Fig. 4*) depends on the ratio between the elastic support c_v and the longitudinal stiffness of the screw. An approximately triangle-shaped distribution of the normal force leads to buckling of the screw close to the screw head.

Taking into account the elastic foundation c_h and the elastic support c_v , the buckling loads for screws as reinforcements were calculated by a finite element calculation. Thereby, a clamped screw head support and a hinged screw head support were modelled.

A hinged screw head support must be assumed, when the surface of the screw heads is flush with the beam surface. In this case, using a steel plate, loads from the beam support can be transferred simultaneously into the timber and into the screws. A clamped screw head support may only be assumed by clamping the screw heads i.e. in the steel plate. For this, it is necessary to countersink the steel plate in the form of the screw heads in such a way as the surface of the screw heads is flush with the lower steel plate surface.

The buckling loads were derived depending on the screw length and on the density of the timber, for hinged and clamped screw head supports, with $E_S = 210000 \text{ N/mm}^2$ and with a ratio between the core and the thread diameter of $d_k/d = 0,7$ (see *Tab. 1 and 2*).

Tab. 1: Characteristic buckling loads for hinged screw head supports

$N_{ki,G,k}$ [kN]	$\rho_k = 310 \text{ kg/m}^3$					$\rho_k = 380 \text{ kg/m}^3$					$\rho_k = 410 \text{ kg/m}^3$					$\rho_k = 450 \text{ kg/m}^3$				
	Screw diameter [mm]					Screw diameter [mm]					Screw diameter [mm]					Screw diameter [mm]				
	4	6	8	10	12	4	6	8	10	12	4	6	8	10	12	4	6	8	10	12
20	3,99	4,51	4,95	5,37	5,79	4,85	5,52	6,06	6,58	7,10	5,22	5,95	6,54	7,10	7,66	5,70	6,53	7,18	7,79	8,40
40	7,50	12,5	14,5	15,9	17,3	8,38	14,9	17,6	19,5	21,1	8,73	16,0	19,0	21,0	22,8	9,16	17,3	20,7	23,0	25,0
60	7,44	16,4	24,2	28,3	31,2	8,30	18,4	28,7	34,3	38,1	8,64	19,2	30,5	36,8	41,0	9,08	20,2	32,7	40,1	44,8
80	7,41	16,5	28,5	39,0	45,4	8,24	18,5	32,2	45,9	54,7	8,58	19,2	33,6	48,7	58,6	9,00	20,2	35,4	52,1	63,7
100		16,6	29,0	43,9	56,9		18,6	32,5	49,7	66,7		19,3	34,0	52,1	70,6		20,3	35,8	55,0	75,4
120			29,4	44,9	62,4			33,0	50,6	71,1			34,4	52,9	74,5			36,2	55,8	78,8
140			29,7	45,7	64,2			33,2	51,4	72,5			34,6	53,7	75,9			36,4	56,7	80,2
160				46,4	65,4				52,1	73,9				54,3	77,3				57,2	81,6
180				46,8	66,5				52,4	75,0				54,7	78,4				57,6	82,7
200			29,8		67,4			33,3		75,8			34,7		79,2					83,5
220				47,1	68,1				52,7	76,4				55,0	79,7				57,8	84,0
>240					68,6					76,9					80,2					84,4
$N_{kl,k}^{1)}$	6,81	16,1	29,9	48,6	72,6	7,54	17,8	33,1	53,8	80,4	7,83	18,5	34,3	55,9	83,5	8,20	19,4	36,0	58,5	87,5

Tab. 2: Characteristic buckling loads for clamped screw head supports

$N_{ki,E,k}$ [kN]	$\rho_k = 310 \text{ kg/m}^3$					$\rho_k = 380 \text{ kg/m}^3$					$\rho_k = 410 \text{ kg/m}^3$					$\rho_k = 450 \text{ kg/m}^3$				
	Screw diameter [mm]					Screw diameter [mm]					Screw diameter [mm]					Screw diameter [mm]				
	4	6	8	10	12	4	6	8	10	12	4	6	8	10	12	4	6	8	10	12
20	13,3	16,9	18,5	20,0	21,6	14,5	20,7	22,6	24,6	26,5	15,0	22,4	24,4	26,5	28,6	15,7	24,6	26,8	29,1	31,3
40	16,2	24,5	36,1	39,1	42,2	19,1	28,2	44,2	47,9	51,7	20,3	29,8	47,7	51,7	55,8	21,7	32,0	50,8	56,8	61,2
60	17,2	31,9	41,1	56,4	62,7	19,3	38,0	48,4	64,4	76,9	20,1	40,5	51,5	67,8	82,9	21,2	43,7	55,6	72,3	91,0
80	17,2	36,6	51,2	61,7	76,5	19,1	41,2	61,4	73,3	89,1	19,8	43,0	65,6	78,2	94,5	20,8	45,3	71,2	84,8	102
100		36,9	60,7	73,9	85,7		41,7	69,5	88,9	102		43,6	72,8	95,2	110		46,0	77,0	103	119
120			62,1	86,8	99,8			70,5	102	120			74,0	108	129			78,4	115	140
140			63,7	92,2	115			72,3	105	137			75,7	111	146			80,0	117	157
160				94,5	126				108	145				114	153				121	163
180	15,6			97,2	130				111	149				116	157				123	167
200		36,1			134					154					162					172
220			64,8		137			73,0		157			76,2		165				124	175
>240				99,1	140				112	159				117	167					177
$N_{ki,k}^{(2)}$	13,6	32,1	59,7	97,2	145	15,1	35,6	66,1	108	161	15,7	37,0	68,7	112	167	16,4	38,7	72,0	117	175

Useful for comparison, the buckling loads $N_{ki,k}^{(1)}$ and $N_{ki,k}^{(2)}$ are displayed in the bottom line in Tab. 1 and Tab. 2. Here, $N_{ki,k}^{(1)} = \sqrt{c_h \cdot E_S \cdot I_S}$ corresponds to the buckling load for elastically bedded beams without supports (Zimmermann, 1905). The buckling load for elastically bedded beams on two supports can be calculated by $N_{ki,k}^{(2)} = 2 \cdot \sqrt{c_h \cdot E_S \cdot I_S}$ (Engesser, 1884). For slender and long beams, $N_{ki,k}^{(1)}$ and $N_{ki,k}^{(2)}$ is independent of the beam length. Subject to these limitations, the buckling load for long screws can be easily calculated using $N_{ki,k}^{(1)}$ or $N_{ki,k}^{(2)}$, $E_S = 210000 \text{ N/mm}^2$ and $I_S = \frac{\pi}{64} \cdot (0,7 \cdot d)^4$.

2.4 Load distribution in beam supports

The load-carrying capacity for the third failure mode is characterised by reaching the compressive strength perpendicular to the grain in a plane formed by the screw tips. In this case, the load-carrying capacity for this failure mode depends on the compressive strength perpendicular to the grain and on the compressed area in a plane formed by the screw tips. The load distribution and consequently the length of the plane formed by the screw tip where compressive stresses occur were determined from a numerical calculation (see [2]). Two different beam supports were studied: Directly loaded sleepers and indirectly loaded beam supports.

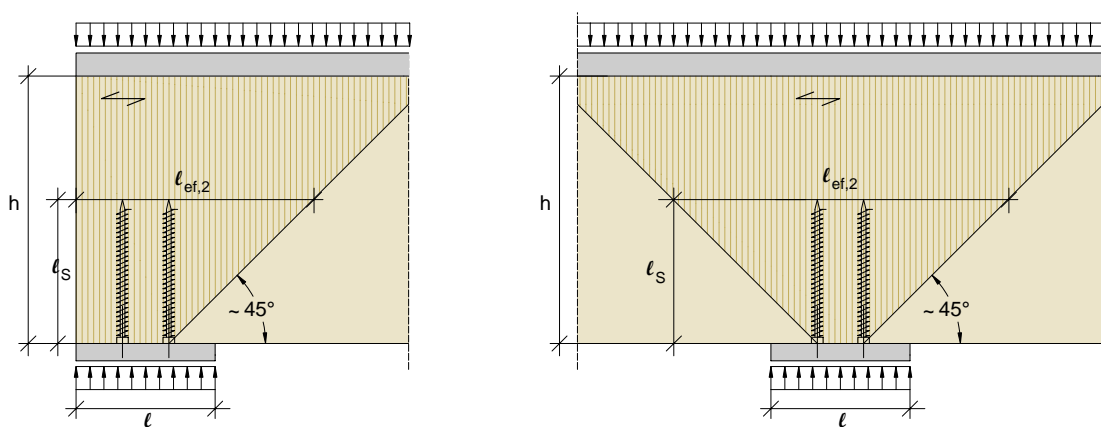


Fig. 5: Load distribution in directly loaded beam supports

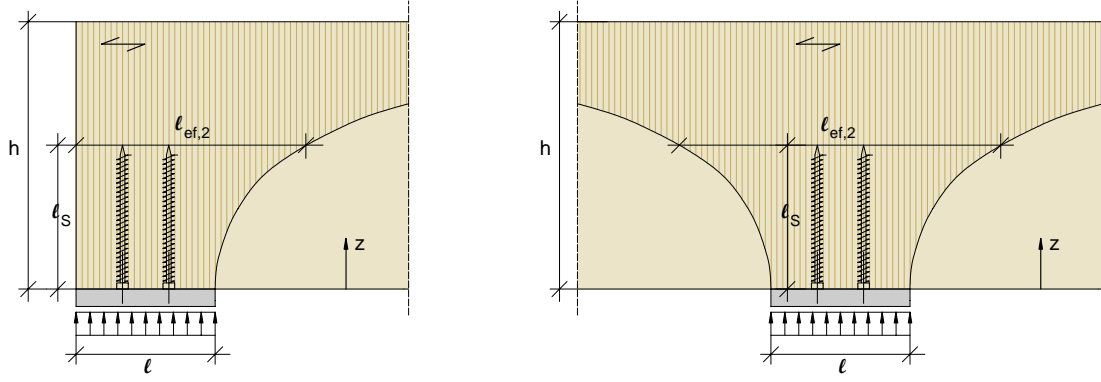


Fig. 6: Load distribution in indirectly loaded beam supports

In directly loaded sleepers a linear load distribution may approximately be assumed (see in Fig. 5). The length of the plane formed by the screw tips where compressive stresses occur can be calculated taking into account the length of the screws and the length of the beam support. In contrast, the load distribution in indirectly loaded beam supports is nonlinear and the increase becomes less with increasing beam height (see in Fig. 6).

As a result of the nonlinear load distribution in indirectly loaded beam supports (see in Fig. 6), the length of the plane formed by the screw tips where compressive stresses occur can be calculated as follows. For single-sided load distribution see eq. (4), for double-sided load distribution see eq. (5).

$$\ell_{ef,2} = \ell + 0,25 \cdot \ell_s \cdot e^{3,3 \cdot \frac{\ell_s}{h}} \quad (4)$$

$$\ell_{ef,2} = \ell + 0,58 \cdot \ell_s \cdot e^{3,6 \cdot \frac{\ell_s}{h}} \quad (5)$$

2.5 Design equations for the load-carrying capacity of reinforced beam supports

Taking into account the three different failure modes, the load-carrying capacity $R_{90,d}$ of a reinforced beam support may be calculated as follows:

$$R_{90,d} = \min \left\{ \begin{array}{l} n \cdot R_d + k_{c,90} \cdot \ell_{ef} \cdot b \cdot f_{c,90,d} \\ b \cdot \ell_{ef,2} \cdot f_{c,90,d} \end{array} \right\} \quad (6)$$

where

$$R_d = \min \{ R_{ax,d} ; R_{c,d} \} \quad (7)$$

$$R_{c,d} = \kappa_c \cdot N_{pl,d} \quad (8)$$

$$\kappa_c = 1 \quad \text{for } \bar{\lambda} \leq 0,2$$

$$\kappa_c = \frac{1}{k + \sqrt{k^2 - \bar{\lambda}^2}} \quad \text{for } \bar{\lambda} > 0,2 \quad (9)$$

with

$$k = 0,5 \cdot \left[1 + 0,49 \cdot (\bar{\lambda} - 0,2) + \bar{\lambda}^2 \right] \quad (10)$$

$$\bar{\lambda} = \sqrt{\frac{N_{pl,d}}{N_{ki,d}}} \quad (11)$$

and

$R_{ax,d}$	Design value of the withdrawal capacity (see eq. (1)) calculated with k_{mod} and $\gamma_M = 1,3$.
n	Number of screws
b	Width of the beam
l_{ef}	$l_{ef} = l + \max \{l ; 30 \text{ mm}\}$ for single-sided load distribution, see in [1] $l_{ef} = l + 2 \cdot \max \{l ; 30 \text{ mm}\}$ for double-sided load distribution, see in [1]
$l_{ef,2}$	see in Fig. 5 and 6
$k_{c,90}$	Coefficient $k_{c,90} \in [1 ; 1,75]$ for the load distribution, see in [1]
$f_{c,90,d}$	Design value of the compressive strength perpendicular to the grain
$N_{pl,d}$	Design value of the plastic load-carrying capacity calculated with the cross section of the core diameter of the screw.
$N_{ki,d}$	Design value of the buckling load for a screw taking into account the elastic foundation perpendicular to the screw axis, a triangular normal load distribution along the screw axis as well as the support condition of the screw head. For hinged head supports the design values of the buckling load are summarised in Tab. 1. For clamped head supports see Tab. 2. The design value is calculated from the characteristic value with k_{mod} and $\gamma_M = 1,3$.

3 Calculation model for the stiffness

The effective stiffness perpendicular to the grain in the range of the reinforced beam support is derived using the Volkersen Theory (1953). The complete derivation for the effective stiffness of a reinforced beam support is specified in [2]. The effective stiffness of a reinforced beam support can be estimated by the following equation:

$$E_{tot} = \frac{E_{90} \cdot f_{LD} \cdot n \cdot \ell_s \cdot \left(\frac{\psi}{n} + 1 \right) \cdot \omega \cdot \sinh(\omega \cdot \ell_s)}{\phi - \psi + n \cdot \left(\frac{\psi}{n} + 1 \right) \cdot \cosh(\omega \cdot \ell_s) + 0,7 \cdot f_{LD} \cdot \ell_s \cdot \phi \cdot \omega \cdot \sinh(\omega \cdot \ell_s)} \quad (12)$$

with the load distribution factor f_{LD} for a linear load distribution

$$f_{LD} = \sqrt{1 + L \cdot \frac{\ell_s}{\ell} \cdot \tan \alpha} \quad (13)$$

and with the ratio between the extensional stiffness of the timber and the screw ϕ as well as the coefficient ψ and ω :

$$\phi = \frac{E_{90} \cdot A}{E_S \cdot A_S} \quad \psi = \frac{n + \phi \cdot \cosh(\omega \cdot \ell_s)}{\cosh(\omega \cdot \ell_s) - 1} \cdot f_{LD} \quad \omega = \sqrt{\left(\frac{1}{E_S \cdot A_S} + \frac{n}{E_{90} \cdot A} \right) \cdot c_v} \quad (14)$$

Further notation:

n	Number of screws
$E_{90} \cdot A$	extensional stiffness of the beam at the beam support perpendicular to the grain direction
$E_S \cdot A_S$	extensional stiffness of the reinforcing screw
c_v	see eq. (3)
$l_S, l, \alpha = 45^\circ$	see in Fig. 5
L	$L = 1$ for single-sided, $L = 2$ for double-sided load distribution

It must be pointed out, that the effective stiffness estimated by eq. 12 to 14 is only valid for reinforced beam supports using self-tapping screws. Furthermore, the equations only apply for a linear load distribution, such as in directly loaded beam supports. The effective stiffness for reinforced beam supports in the range of the reinforcing screws is only valid, when the surface of the screw heads is exactly flush with the surface of the beam support. To receive an impression about the size of E_{tot} depending on the reinforcement, two diagrams were generated. Left in Fig. 7 the effective stiffness depending on the screw number n and the screw length l_S is displayed for a screw with 6 and 12 mm diameter. Remarkable is the increasing of E_{tot} with increasing screw length. Right in Fig. 7 the effective stiffness depending on the beam support area and the screw diameter for one screw ($n = 1$) is displayed. Remarkable is the increase of E_{tot} with decreasing spacing between the screws. For large screw spacing, E_{tot} is hardly higher than the MOE for solid timber perpendicular to the grain.

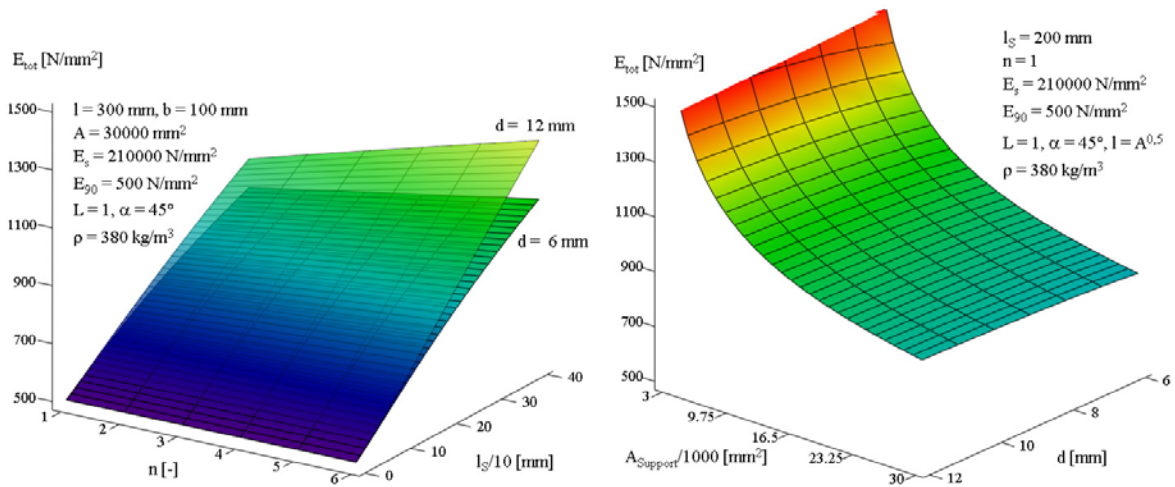


Fig. 7: E_{tot} depending on l_S and n (left) and E_{tot} depending on A and d (right)

4 Tests

To verify the calculation models, different reinforced beam supports were tested (15 test series). To demonstrate the effectiveness of reinforced beam supports, further non-reinforced beam supports were tested (4 test series). All tested specimens are specified in Tab. 3. The averaged load-carrying capacity for each test series is displayed in column four. In the following column the averaged effective stiffness of the reinforced beam supports is displayed. Information about the geometry of the beam support and the screws as well as the plastic load-carrying capacity N_{pl} for the screws are displayed in column 6 to 12.

A remarkable effect of this reinforcing method is the high increase in load-carrying capacity compared to the non-reinforced geometrically identical beam supports. For example, the averaged load-carrying capacity for the test series A_6_6 is 132 kN and consequently 130% higher than the corresponding value for the test series A_2. The greatest increase in load-carrying capacity was reached with the test series D_8b_6. Here, compared to the test series D_2, the increase in load-carrying capacity was 330%.

Furthermore, for reinforced beam supports a high increase in stiffness perpendicular to the grain direction is observed. Compared to solid timber with a MOE perpendicular to the grain of about 300 – 500 N/mm², the effective stiffness E_{tot} perpendicular to the grain in the range of the reinforcing screws reached a maximum value of about 1870 N/mm².

Tab. 3: Properties of tested beam supports and test results

specimen	number of spec.	mean density	mean load-carrying capacity	mean MOE	beam support			reinforcing screws			
					direct/indirect	width	length	number of screws	screw diameter	length of the threaded part	ductile axial force
[-]	n	ρ	R_{90}	E_{tot}	[-]	t	l_{ef}	n	d	l_s	N_{pl}
		[kg/m ³]	[kN]	[N/mm ²]		[mm]	[mm]	[-]	[mm]	[mm]	[kN]
A_1	5	463	43,2	-	indirekt	100	80	-	-	-	-
A_7_2	5	444	77,5	790	indirect	100	80	2	7,5	180	32,7
A_8_2	5	459	92,0	1293	indirect	100	80	2	8	340	32,7
A_10_2	5	448	104	845	indirect	100	80	2	10	200	51,8
A_7_4	4	446	126	635	indirect	100	120	4	7,5	180	32,7
A_10_4	5	449	133	764	indirect	100	120	4	10	200	51,8
A_2	10	464	57,1	-	indirekt	120	90	-	-	-	-
A_6_6	10	466	132	861	indirect	120	90	6	6,5	115/160	22,5
D_1	5	451	46,0	-	direkt	100	80	-	-	-	-
D_7_2	5	460	96,1	1050	direct	100	80	2	7,5	180	34,2
D_8_2	5	425	98,0	1350	direct	100	80	2	8	340	32,7
D_10_2	5	439	104	1119	direct	100	80	2	10	200	51,8
D_7_4	14	443	127	985	direct	100	120	4	7,5	180	34,2
D_8_4	6	445	169	1247	direct	100	120	4	8	340	32,7
D_10_4	5	456	173	836	direct	100	120	4	10	200	51,8
D_2	3	450	56,4	-	direkt	120	90	-	-	-	-
D_7_6	3	459	195	1196	direct	120	90	6	7,5	180	34,2
D_8a_6	3	453	228	1435	direct	120	90	6	8	260	39,1
D_8b_6	3	455	242	1870	direct	120	90	6	8	400	37,5

In the following Fig. 8 and Fig. 9 the test results (R_{90} and E_{tot}) for each test series are compared with the calculated values. All values were calculated with the averaged density and the averaged plastic load-carrying capacity for the screws. Furthermore, the compressive strength perpendicular to the grain was assumed as 5 N/mm². The effective stiffness perpendicular to the grain E_{tot} was calculated using a MOE of 300 N/mm².

The calculated values show a good agreement with the test results. Furthermore, the calculated failure modes mainly correspond to the failure modes observed in the tests (see in Fig. 8).

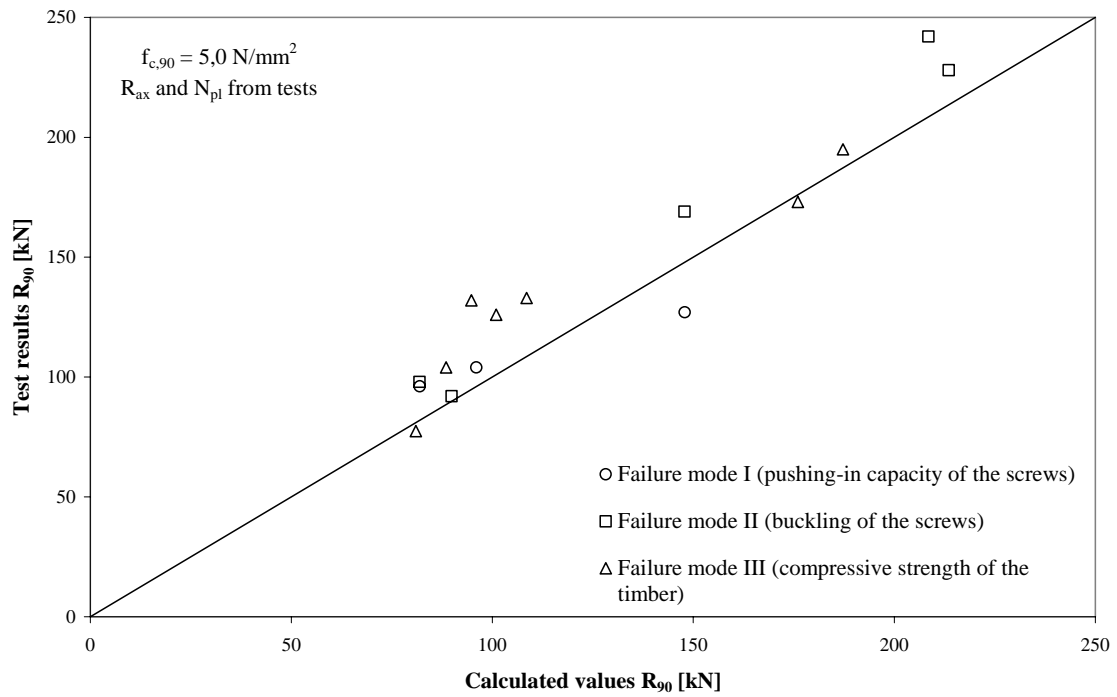


Fig. 8: Calculated load-carrying capacities in comparison with the test results

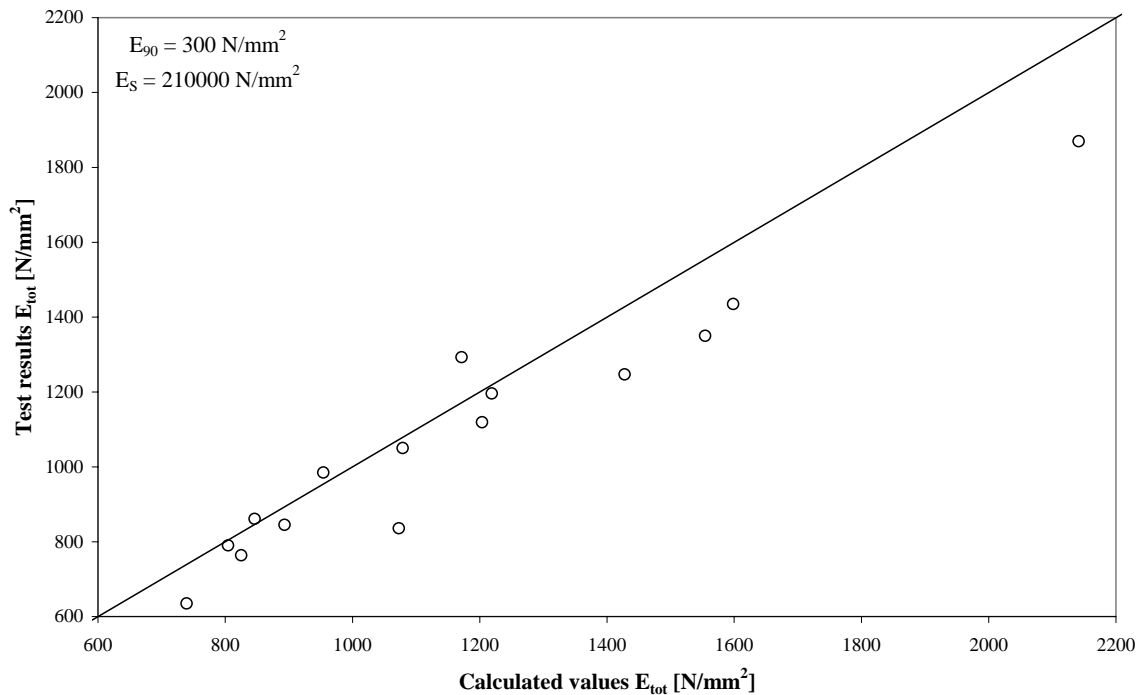


Fig. 9: Calculated effective stiffness in comparison with the test results

5 Summary

Self-tapping screws with continuous threads provide a good opportunity to reinforce beam supports and consequently to increase the load-carrying capacity and the stiffness perpendicular to the grain or to minimize the elastic displacement perpendicular to the grain. In this paper a calculation model for the load-carrying capacity and for the effective stiffness reinforced beam supports using self-tapping screws is presented. With the first calculation model it is possible to calculate the load-carrying capacity and to predict the failure mode of a reinforced beam support. The second calculation model may be used to estimate the stiffness or the elastic displacement perpendicular to the grain in the support area. Both calculation models were verified by test.

6 References

- [1] DIN 1052:2004-08, Entwurf, Berechnung und Bemessung von Holzbauwerken – Allgemeine Bemessungsregeln und Bemessungsregeln für den Hochbau
- [2] Bejtka, I. (2005). Verstärkung von Bauteilen aus Holz mit Vollgewindeschrauben. Band 2 der Reihe Karlsruher Berichte zum Ingenieurholzbau. Herausgeber: Universität Karlsruhe (TH), Lehrstuhl für Ingenieurholzbau und Baukonstruktionen, Univ.-Prof. Dr.-Ing. H.J. Blaß. ISSN 1860-093X, ISBN 3-937300-54-6
- [3] Volkersen, O. (1953). Die Schubkraftverteilung in Kleb-, Niet- und Bolzenverbindungen. Aus Energie und Technik, March.1953
- [4] Blaß, H.J.; Görlacher, R. (2004). Compression perpendicular to the grain. In proceedings of the 8th World Conference on Timber Engineering – Volume II, page 435 – 440; WCTE 2004, June 14-17, 2004 in Lahti, Finland